JACS
JOURNAL OF THE AMERICAN CHEMICAL SOCIETY

Article

pubs.acs.org/JACS

Reactions of Boron-Derived Radicals with Nucleophiles

Lauren E. Longobardi,[†] Pavel Zatsepin,[†] Roman Korol,[†] Lei Liu,[‡] Stefan Grimme,[‡] and Douglas W. Stephan*[,†]

[†]Department of Chemistry, University of Toronto, 80 St. George Street, Toronto, Ontario M5S 3H6, Canada

[‡]Mulliken Center for Theoretical Chemistry, Institut fuer Physikalische und Theoretische Chemie, Universitaet Bonn, Beringstrasse 4, D-53115 Bonn, Germany

Supporting Information

ABSTRACT: Reactions of phenanthrenedione- and pyrenedione-derived borocyclic radicals, $C_nH_8O_2B(C_6F_5)_2^{\bullet}$ (n = 14 (**1**), 16 (**3**)), with a variety of nucleophiles have been studied. Reaction of **1** with P(t-Bu)$_3$ affords the zwitterion 3-(t-Bu)$_3$P$C_{14}H_7O_2B(C_6F_5)_2$ (**5**) in addition to the salt [HP(t-Bu)$_3$][$C_{14}H_8O_2B(C_6F_5)_2$] (**6**). In contrast, the reaction of **1** with PPh_3 proceeds to give two regioisomeric zwitterions, 1-(Ph_3P)$C_{14}H_7O_2B(C_6F_5)_2$ (**7a**) and 3-(Ph_3P)$C_{14}H_7O_2B(C_6F_5)_2$ (**7b**), as well as the related boronic ester $C_{14}H_8O_2B(C_6F_5)$ (**2**). In a similar fashion, **3** reacted with PPh_3 to give 3-(Ph_3P)$C_{16}H_7O_2B(C_6F_5)_2$ (**8a**), 1-(Ph_3P)$C_{16}H_7O_2B(C_6F_5)_2$ (**8b**), and boronic ester $C_{16}H_8O_2B(C_6F_5)$ (**4**). Reactions of secondary phosphines Ph_2PH and tBu_2PH with **3** yield 3-(R_2PH)$C_{16}H_7O_2B(C_6F_5)_2$ (R = Ph (**9**), t-Bu (**10**)). The reaction of **1** with N-heterocyclic carbene IMes afforded 3-(IMes)$C_{14}H_7O_2B(C_6F_5)_2$ (**11**) and [IMesH][$C_{14}H_8O_2B(C_6F_5)_2$] (**12**), while the reactions with quinuclidine and DMAP afforded the species 3-($C_7H_{13}N$)$C_{14}H_7O_2B(C_6F_5)_2$ (**13**) and [H(NC_7H_{13})$_2$][$C_{14}H_8O_2B(C_6F_5)_2$] (**14**), and the salt [9,10-(DMAP)$_2C_{14}H_8O_2B(C_6F_5)_2$][$C_{14}H_8O_2B(C_6F_5)_2$] (**15**), respectively. These products have been fully characterized, and the mechanism for the formation of these products is considered in the light of DFT calculations.

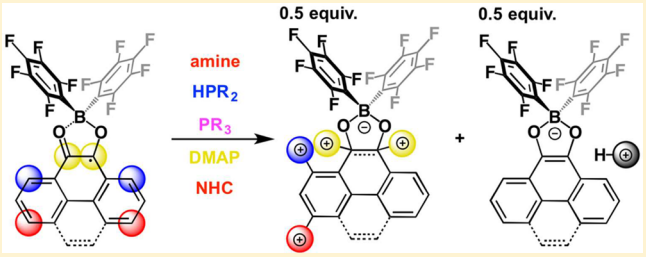

INTRODUCTION

Since the early work of Gomberg[1] and others,[2] carbon-based radicals have been studied as intermediates in various transformations, including polymerizations,[3] reductions, and cyclizations.[4,5] Studies have also revealed the importance of hydroxyl radicals in atmospheric chemistry.[6,7] Oxygen-based radicals are critical in biology,[8] participating in cell signaling mechanisms and metabolism and effecting cell damage that is involved in diseases such as cancers, stroke, heart disease, and diabetes. Despite these broad and diverse roles of radicals, a majority of paramagnetic systems studied to date have been transition metal based.[9] It is noted that studies describing boron-containing radicals have garnered recent attention,[10] but explorations of their chemistry remain rare.

Electrochemical reductions provide an avenue for the generation of boron containing radicals. For example, the radical derived from reduction of p-$C_6H_4(BMes_2)_2$ was reported by Kaim[11−13] and crystallographically characterized by Marder,[14] while similar treatment of the Cr complexes ($Mes_{3-n}B(\eta^6$-$C_6H_3Me_3)_n(Cr(CO)_3)_n$ gave B-centered radicals.[15]

Chemical reductions have also been used extensively to obtain boron-containing free radicals. Power and co-workers prepared $[BMes_3]^{\bullet-}$ by reduction with Li^0 and obtained the first molecular structure of a boron-centered radical by sequestration with 12-crown-4.[16] In 2011 Norton reported the generation of the short-lived anionic species $[B(C_6F_5)_3]^{\bullet-}$ by reducing $B(C_6F_5)_3$ with $Co(Cp^*)_2$.[17] Similarly, the syntheses of persistent trialkylboron radical anions, $[BR_3]^{\bullet-}$ (R = t-Bu or Np),[18] was achieved. Many recent examples of boron-containing radicals take advantage of π-delocalization to access persistent or stable species. Select examples (Figure 1) include Piers' reduced benzo[c]cinnoline adduct of 2,2′-diborabiphenyl,[19] Jäkle's 1,2-diborylated ferrocene dimer $[CpFeC_5H_3BPh]_2$,[20] Gabbaï's borylated acridine,[21] Nozaki's β-diiminate-based heterocyclic boron radical,[22] Bourissou's phosphine-coordinated boryl radical,[23] Braunschweig's spirocyclic zwitterionic radical,[24] and Marder's boryl-pyrene species.[14]

One-electron reduction of B−B bonds was exploited by Gäbbai[25] to generate the radical anion $[C_{10}H_6(BMes_2)_2]^{\bullet-}$. Bertrand accessed the singlet diradical [t-BuB−PiPr$_2$]$_2$[26] by treating B−B dimer (t-BuBCl)$_2$ with LiP(i-Pr)$_2$. More recently, Wagner and co-workers[27] have described a related strategy exploiting the proximity of two boron atoms to stabilize a boron radical via the one electron B−B bonded radical anion $[(C_{10}H_4B)_2CHCH_2C(CH_3)_3]^{\bullet}$. Related work by Braunschweig described the oxidation of a B═B bond to generate boron radical cations.[28,29]

In the past few years, another strategy to stabilize boron derived radicals has been to employ carbene donors.[30] Curran and Lacôte have reported applications of their NHC-stabilized

Received: October 26, 2016
Published: November 30, 2016

DOI: 10.1021/jacs.6b11190
J. Am. Chem. Soc. 2017, 139, 426−435

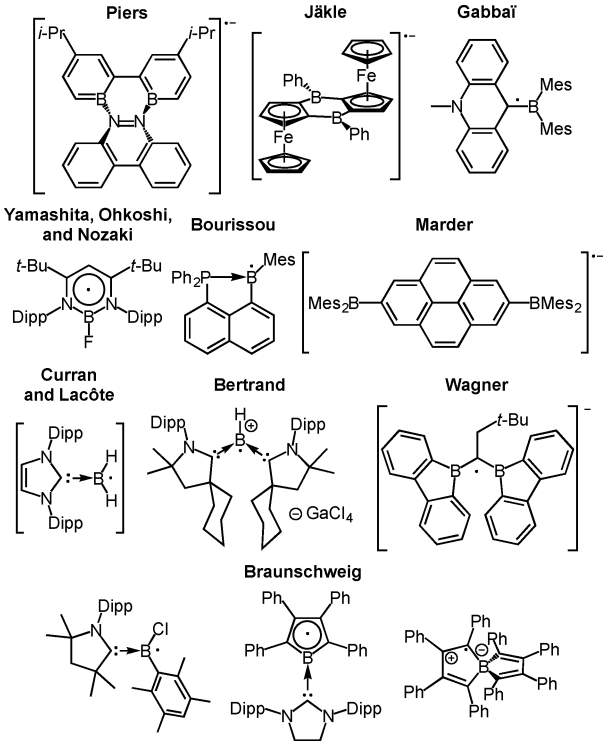

Figure 1. Examples of boron-containing radicals.

boron-centered radicals $[(NHC)BH_2]^{\bullet}$[31,32] and $[(NHC)BHPh]^{\bullet}$.[33] Bertrand[34] has exploited the more π-acidic cyclic alkyl amino carbenes (CAACs) to prepare the cationic radical $[(CAAC)_2BH]^{\bullet+}$,[35] while Braunschweig has reported the syntheses of an NHC-stabilized borole radical[36] and the CAAC-stabilized boron radical $[(CAAC)BHDur]^{\bullet}$.[37]

Frustrated Lewis pair (FLP) chemistry has also been applied to access paramagnetic systems. Our group reported C−H activation by transient P/Al "frustrated radical pairs" derived from the reaction of a P/Al FLP adduct of N_2O.[38] Subsequently, Erker has described radical polymerizations mediated by boron-containing radicals derived from the reaction of NO with intramolecular FLPs.[39−42] More recently, combinations of TEMPO and boranes have been shown to effect H_2 cleavage[43,44] and FLP additions to alkenes. In our own work,[45] we have exploited FLP H_2 activation using 9,10-phenanthrenedione and 4,5-pyrenedione to access the corresponding boron-derived radicals $C_nH_8O_2B(C_6F_5)_2^{\bullet}$ (n = 14 (**1**), 16 (**3**)) and the boronic ester byproducts **2** and **4**, respectively (Scheme 1). These remarkably air-stable radicals can be reduced to their corresponding borate anions, and

Scheme 1. FLP-Reduction of Aromatic Diones to Borocyclic Radicals and Boronic Esters

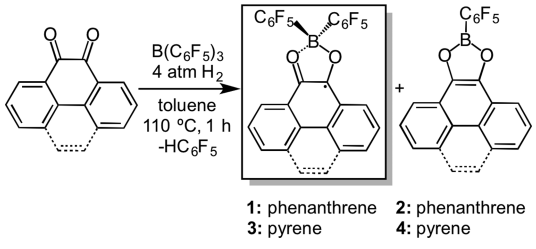

computational studies of the spin density and SOMO suggest the free electron is delocalized over the aromatic scaffold.

The majority of studies of boron-containing radicals have focused on generation and characterization of such species, while subsequent reactivity has drawn little attention. In this manuscript, the reactivity of radicals **1** and **3** with a series of nucleophiles, including tertiary and secondary phosphines, carbenes, and amines is presented. The unique products are fully characterized, and the mechanistic implications are considered.

RESULTS AND DISCUSSION

Reactions of borocyclic radicals $C_{14}H_8O_2B(C_6F_5)_2^{\bullet}$ (**1**) and $C_{16}H_8O_2B(C_6F_5)_2^{\bullet}$ (**3**) with $PMes_3$ were undertaken with the intent to effect reduction to the corresponding radical cation $[PMes_3]^{\bullet+}$ and borate anion. After several hours at room temperature in d_8-toluene, very little starting material had been consumed (as evidenced by multinuclear NMR data), and a small amount of degradation was observed, based on the detection of $[HPMes_3]^+$. This prompted trials with other phosphines. The reaction of **1** with 1 equiv of P(t-Bu)$_3$ in CD_2Cl_2 led to the formation of two new species, as evidenced by ^{31}P NMR spectroscopy. One species, **5**, gave rise to a singlet at 49 ppm, and a second species, **6**, resonated as a doublet centered at 60 ppm (J = 430 Hz), which collapsed to a singlet in the $^{31}P\{^1H\}$ NMR spectrum. The reaction mixture also changed from an initial dark black-yellow color to a vibrant yellow color over the course of the reaction. Crystals grown from the NMR scale reaction were suitable for X-ray diffraction analysis, and the data revealed the molecular structure of a diamagnetic zwitterionic species 3-(t-Bu)$_3$P$C_{14}H_7O_2B(C_6F_5)_2$, **5** (Figure 2a). In this molecule, P(t-Bu)$_3$ is bound to the 3-

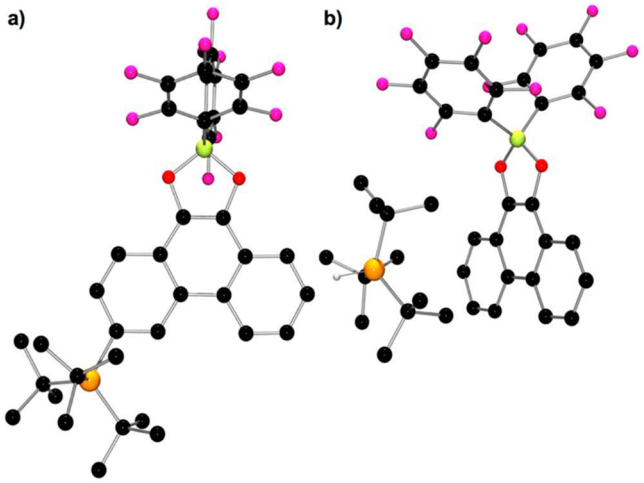

Figure 2. POV-ray depiction of (a) **5** and (b) **6**, with carbon-bound H atoms omitted for clarity. C, black; B, yellow-green; F, pink; O, red; P, orange.

position of the phenanthrene backbone. The P−C(3) bond of 1.826(2) Å is canted slightly out of the plane of the phenanthrene ring, with a P−C(3)-C(2)−C(1) dihedral angle of 169.1(2)°. Multinuclear NMR data of the crude reaction mixtures suggested that the second species formed from the reaction of **1** with P(t-Bu)$_3$ is the salt $[HP(t\text{-}Bu)_3][C_{14}H_8O_2B(C_6F_5)_2]$, **6** (Scheme 2).[46,47] While isolating **6** from **5** was not possible, single crystals of **6** grew from a mixture of the two compounds, and X-ray diffraction analysis structurally con-

DOI: 10.1021/jacs.6b11190
J. Am. Chem. Soc. 2017, 139, 426−435

Scheme 2. Reactions of 1 with Phosphines To Give 5−7

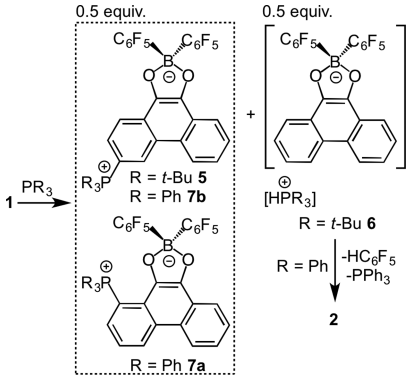

firmed the identity of this byproduct (Figure 2b). Compound **5** was isolated in 66% yield via purification by column chromatography.

The analogous reaction of **1** with PPh_3 in d_8-toluene at room temperature also led to a color change from dark black-yellow solution to a cloudy yellow-orange mixture, although this reaction progressed more slowly than that of **1** with $P(t\text{-}Bu)_3$. The ^{31}P NMR spectrum revealed the formation of two new products, **7a** and **7b**, which gave rise to singlet resonances at 29 and 23 ppm, respectively. In addition, free PPh_3 was observed spectroscopically. The ^{11}B NMR spectrum of the reaction mixture showed two broad resonances at 29 and 10 ppm. The characteristic resonances of HC_6F_5 were observed in the ^{19}F NMR spectrum. This latter observation, in addition to the ^{11}B NMR resonance at 29 ppm and the observation that a sparingly soluble, white precipitate formed during the reaction, suggested that boronic ester $C_{14}H_8O_2B(C_6F_5)$, **2**, which has been previously characterized,[45] was formed. Red-orange crystals were grown from the reaction mixture, and X-ray diffraction analysis confirmed the identity as zwitterion 1-(Ph_3P)-$C_{14}H_7O_2B(C_6F_5)_2$, **7a** (Figure 3a), where PPh_3 is bound to the 1-position of the phenanthrene ring. This material gives rise to the ^{31}P NMR resonance at 29 ppm. Work-up and flash column chromatography afforded the clean separation of the two phosphorus-containing products from **2**. The product that gives rise to a resonance at 23 ppm in the ^{31}P NMR spectrum

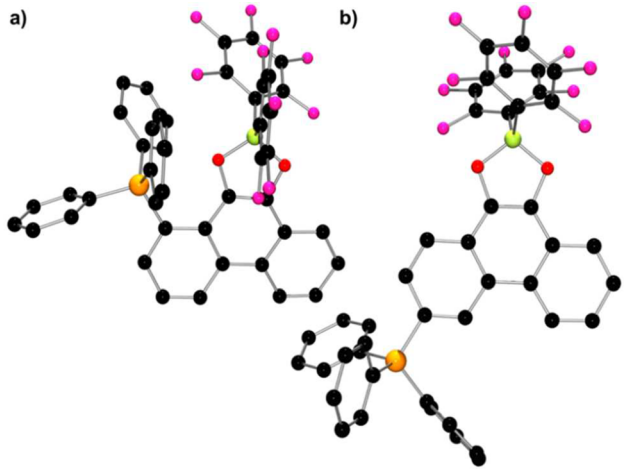

Figure 3. POV-ray depictions of (a) **7a** and (b) **7b**; H atoms are omitted for clarity. C, black; B, yellow-green; F, pink; O, red; P, orange.

was isolated as a yellow precipitate. Recrystallization from toluene at −35 °C afforded yellow crystals, which X-ray diffraction analysis revealed to be zwitterion 3-(Ph_3P)-$C_{14}H_7O_2B(C_6F_5)_2$, **7b** (Figure 3b), where PPh_3 is bound to the 3-position of the phenanthrene ring. The P−C(1) bond length in **7a** is 1.800(2) Å, whereas the P−C(3) bond length in **7b** is 1.783(2) Å. The overall reaction (Scheme 2) is proposed to proceed in similar fashion to that of $P(t\text{-}Bu)_3$, however the $[HPPh_3]^+$ cation is sufficiently acidic[48] to protonate a C_6F_5 ring of the transient borate, liberating the boronic ester, HC_6F_5, and PPh_3. Thus, 1 equiv of **1** consumes a substoichiometric amount of PPh_3.

Analogous chemistry was observed with radical **3**. Treatment with substoichiometric amounts of PPh_3 afforded a raspberry colored $CDCl_3$ solution of **8a** and **8b**, HC_6F_5, and boronic ester **4**. The two new phosphorus containing products give rise to resonances at 29 and 22 ppm in the ^{31}P NMR spectrum. While the majority of **4** was removed by filtration, the two phosphorus-containing products were separated and purified by preparative TLC. Single crystals of both products were grown, and X-ray diffraction analysis confirmed their identities as zwitterions 3-$(Ph_3P)C_{16}H_7O_2B(C_6F_5)_2$ (**8a**) and 1-(Ph_3P)-$C_{16}H_7O_2B(C_6F_5)_2$ (**8b**), where PPh_3 is bound at the 3-position and 1-position of the pyrene ring, respectively (Scheme 3).

Scheme 3. Reactions of 3 with PPh_3, $HPPh_2$, and $HP(t\text{-}Bu)_2$ To Give 8−10

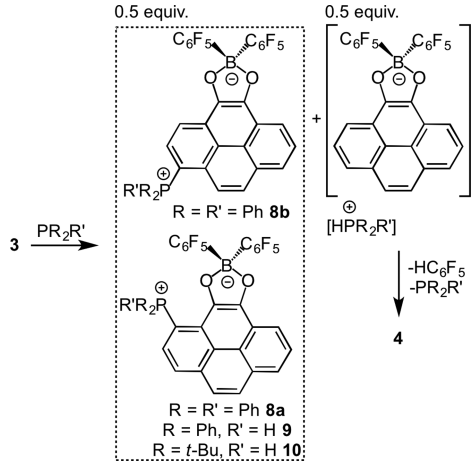

Both species are highly colored: **8a** is a bright orange color and **8b** is a bright pink color when dissolved in various organic solvents. The new P−C bonds in **8a** and **8b** were found to be 1.795(2) Å and 1.778(5) Å, respectively (Figure 4).

The reaction of $HPPh_2$ with radical **3** (Scheme 3) resulted in the loss of HC_6F_5 and formation of boronic ester **4**, and a new phosphorus containing product **9** was generated, as evidenced by a doublet centered at 6 ppm in the ^{31}P NMR spectrum (J = 547 Hz). Single crystal X-ray diffraction of **9** confirmed its identity as the zwitterion 3-$(Ph_2PH)C_{16}H_7O_2B(C_6F_5)_2$ (Figure 5a), where the $HPPh_2$ substituent is bound at the 3-position on the pyrene scaffold. In a similar fashion, reaction of $HP(t\text{-}Bu)_2$ with **3** afforded 3-$((t\text{-}Bu)_2PH)C_{16}H_7O_2B(C_6F_5)_2$, **10** (Scheme 3), with its molecular structure confirmed crystallographically (Figure 5b). The new P−C bond lengths in **9** and **10** were found to be 1.787(2) and 1.797(3) Å, respectively.

The reaction of **1** with carbon-based nucleophile IMes in THF led to an immediate reaction and a color change from

DOI: 10.1021/jacs.6b11190
J. Am. Chem. Soc. 2017, 139, 426−435

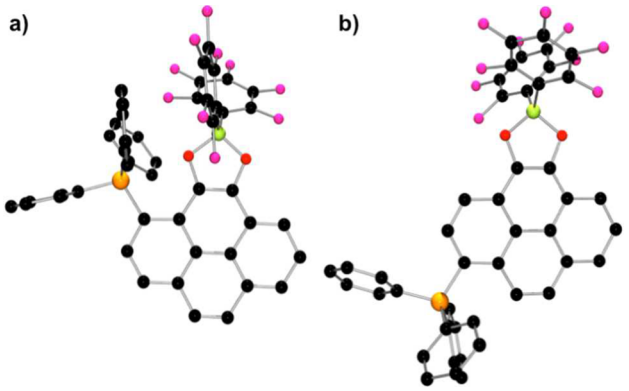

Figure 4. POV-ray depictions of (a) **8a** and (b) **8b**; H atoms are omitted for clarity. C, black; B, yellow-green; F, pink; O, red; P, orange.

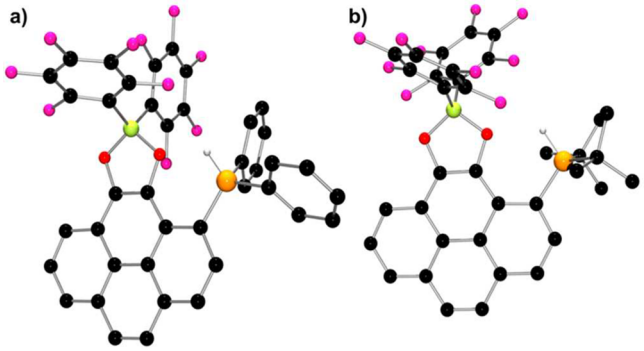

Figure 5. POV-ray depiction of (a) **9** and (b) **10**, with carbon-bound H atoms omitted for clarity. C, black; B, yellow-green; F, pink; H, turquoise; O, red; P, orange.

dark black-yellow to clear yellow (Scheme 4). While this reaction did lead to unidentified byproducts, **11** was isolated as

Scheme 4. Synthesis of 11 and 12

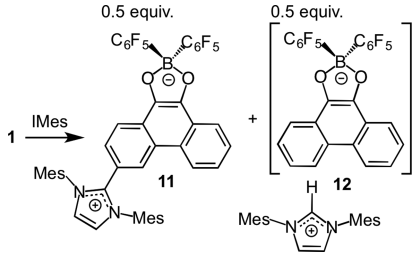

a yellow powder in 68% yield following workup and purification. Recrystallization afforded yellow blocks, which were amenable to X-ray diffraction analysis. This confirmed the identity of **11** as zwitterionic product 3-(IMes)$C_{14}H_7O_2B(C_6F_5)_2$ (Figure 6), where a new C−C bond has formed at the 3-position of the phenanthrene ring. A byproduct of the formation of **11** is presumed to be $[IMesH][C_{14}H_8O_2B(C_6F_5)_2]$, **12** (Scheme 4), in a similar fashion to the reaction of P(*t*-Bu)$_3$ with **1**.

The observations of products derived from P- and C-based nucleophiles led us to explore the reactivity of N-based nucleophiles. The combination of **1** with quinuclidine (quin) proceeds in a fashion analogous to that of P(*t*-Bu)$_3$, resulting in the formation of 3-$(C_7H_{13}N)C_{14}H_7O_2B(C_6F_5)_2$ (**13**) and the

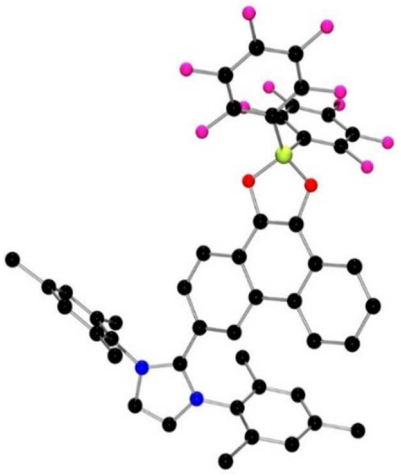

Figure 6. POV-ray depiction of **11**; H atoms are omitted for clarity. C, black; B, yellow-green; F, pink; N, blue; O, red.

byproduct $[H(NC_7H_{13})_2][C_{14}H_8O_2B(C_6F_5)_2]$ (**14**) (Scheme 5). Single crystals of **14** formed from the reaction mixture in

Scheme 5. Synthesis of 13−15

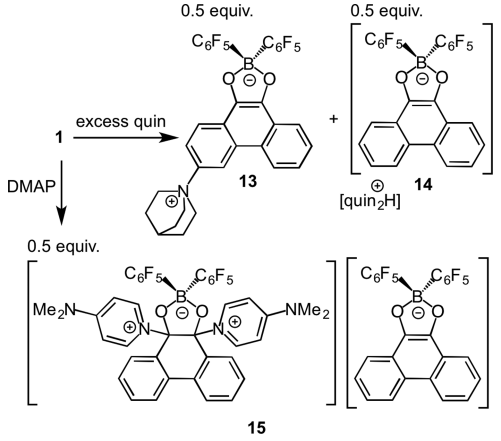

toluene, which were amenable to single crystal X-ray diffraction studies (Figure 7b).[49] After workup and purification, **13** was isolated in 93% yield as a yellow solid, which was recrystallized from THF and hexanes to afford diffraction quality crystals (Figure 7a). **13** was characterized by multinuclear NMR spectroscopy, but **14** degrades in solution, affording HC_6F_5 and what appears to be the quinuclidine adduct of **2** (based on the ^{11}B NMR chemical shift at 11 ppm and the ^{19}F NMR resonances at −129, −156, and −163 ppm in $CDCl_3$). This is presumably a result of the acidic proton from the cation, which promotes the loss of HC_6F_5, akin to that previously seen in the reaction of **1** and **3** with PPh_3, $HPPh_2$, and HP(*t*-Bu)$_2$ (Schemes 2 and 3).

In contrast to the reaction of **1** with quinuclidine, combining **1** with DMAP in toluene resulted in the formation of a large amount of a yellow-orange precipitate, **15** (Scheme 5). The precipitate was collected and dissolved DMSO, and ^{1}H and 2D NMR spectroscopy revealed that, in contrast to the previously discussed reactions, **15** did not show a dissymmetric phenanthrene backbone but rather two different, symmetric phenanthrene units, together with two DMAP units. The ^{19}F NMR spectrum of **15** showed two equivalent C_6F_5 rings, and

DOI: 10.1021/jacs.6b11190
J. Am. Chem. Soc. 2017, 139, 426−435

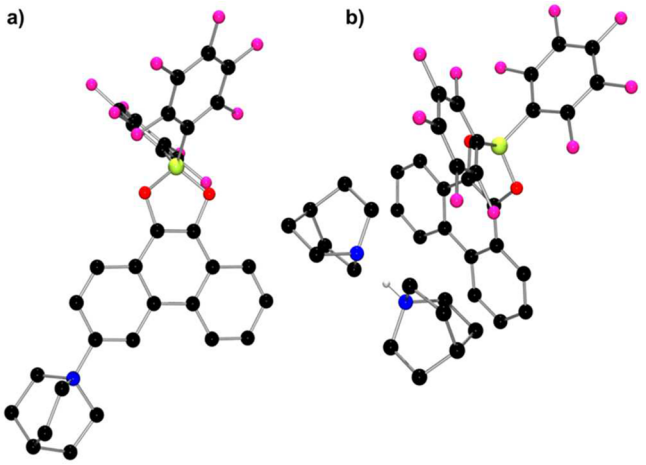

Figure 7. POV-ray depiction of (a) **13** and (b) **14**, with carbon-bound H atoms omitted for clarity. C, black; B, yellow-green; F, pink; N, blue; O, red.

two inequivalent C_6F_5 rings, while the ^{11}B NMR spectrum showed two broad resonances at 10 and 6 ppm. Recrystallization from cold CH_2Cl_2 and subsequent X-ray diffraction analysis of the single crystals confirmed **15** as the salt $[9,10\text{-}(DMAP)_2C_{14}H_8O_2B(C_6F_5)_2][C_{14}H_8O_2B(C_6F_5)_2]$ (Figure 8).

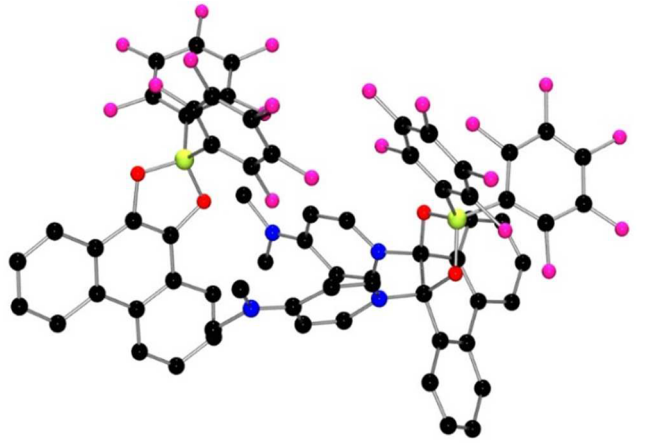

Figure 8. POV-ray depiction of **15**; H atoms omitted for clarity. C, black; B, yellow-green; F, pink; N, blue; O, red.

In the cation, two DMAP molecules are coordinated to the 9- and 10-positions of the phenanthrene ring. This, together with a four-coordinate boron center, affords an overall cationic charge. The counteranion is the same as those found in salts **6**, **14**, and in the previously reported $[CoCp^*_2][C_{14}H_8O_2B(C_6F_5)_2]$.[45] Within the cation, the C−O bond lengths are 1.389(4) and 1.387(5) Å, respectively. The C(9)−N and C(10)−N bond lengths are 1.511(4) and 1.511(5) Å, respectively, and the C(9)−C(10) bond length is 1.571(5) Å, diagnostic of the single bond character, when compared to the C(9)−C(10) bond length in **14** of 1.356(3) Å. The O−C−N angles are 109.5(3)° and 105.5(3)°; O−C(9)C(14) and O−C(10)C(11) angles are 110.0(3)° and 112.9(3)°, respectively; and N−C(9)−C(14) and N−C(10)−C(11) angles are 109.0(3)° and 109.0(3)°, respectively. The C(14)−C(9)−C(10)−C(11) dihedral angle is 36.0(4)°, the O(1)−C(9)−C(10)−O(2) dihedral angle is 37.4(3)°, and the N(3)−C(9)−C(10)−N(1) dihedral angle is 35.6(4)°.

Mechanistic Considerations. Electrochemical studies suggest that **1** and **3** are not sufficiently strong oxidants ($E_{1/2}$ = −0.27 V)[45] to oxidize tertiary or secondary arylphosphines.[50] Furthermore, combinations of **1** with $PMes_3$ did not yield $[PMes_3]^{\bullet+}[C_{14}H_8O_2B(C_6F_5)_2]^-$ after several hours at room temperature (as evidenced by multinuclear NMR data), suggesting that the reaction is not initiated by one-electron transfer from the phosphine nucleophiles to the radicals. The resonance forms of **1** and **3** (Scheme 6), supported by DFT

Scheme 6. Resonance Forms of Radicals 1 and 3

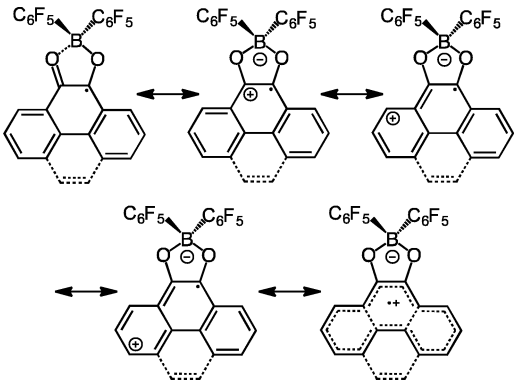

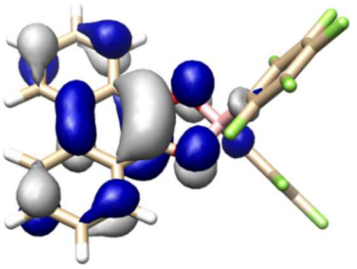

Figure 9. Lowest unoccupied molecular orbital (LUMO) of **1** at a contour surface value of ±0.03 au (PBEh-3c level of theory[51] with Turbomole 7.0 software[52]) (see SI for details).

calculations of the LUMO of **1** (Figure 9), include a zwitterionic borate radical that places cationic charge at the 1-, 3-, 9-, and 10-positions of the phenanthrene system. The electrophilic character of the polyaromatic systems led us to propose an S_NAr mechanism involving nucleophilic attack on the radical π-system. The addition of the nucleophile is thought to prompt electron transfer to a second equivalent of the radical, affording the observed anion, while deprotonation by additional nucleophile affords the countercation and zwitterionic product (Scheme 7). The consumption of a second equivalent of **1** in the reaction with P(*t*-Bu)$_3$ can be circumvented by the addition of a stoichiometric amount of $[FeCp_2][BF_4]$, a one-electron oxidant that is unreactive toward **1**. In this case, the reaction is performed in MeCN to ensure solubility of the ferrocenium salt. This results in the formation of **5** in 62% yield, in addition to $[HP(t\text{-}Bu)_3][BF_4]$ and $FeCp_2$.

The positional selectivity seen for the reactions of the radicals with P(*t*-Bu)$_3$, IMes, and quinuclidine presumably reflects the influence of steric congestion, favoring attack at the less-hindered phenanthrene 3-position and the pyrene 1-position. The formation of **9** and **10** is thought to be selective

DOI: 10.1021/jacs.6b11190
J. Am. Chem. Soc. 2017, 139, 426−435

Scheme 7. Proposed Mechanism of Formation of 5 and 6

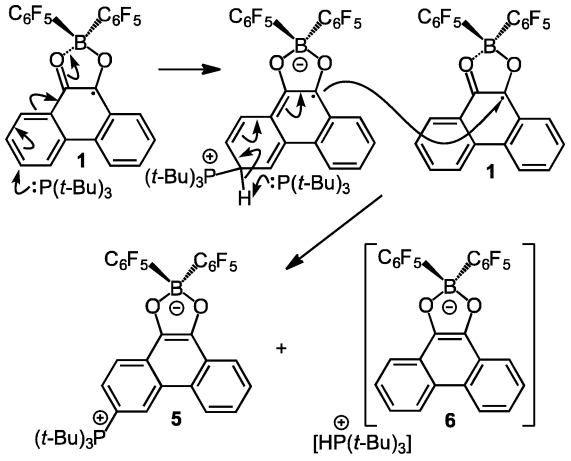

for the pyrene 3-position as a result of H-bonding between the oxygen atoms and the P−H bond. The O···H contacts in the solid state structures of **9** and **10** were found to be 2.43(2) Å and 2.10(2) Å, respectively.

Both solvent and temperature were found to affect the distribution of **7a** and **7b** produced in the reaction of **1** with PPh_3 (Table 1). The barrier for the generation of **7a** is likely larger than the barrier to generate **7b** for steric reasons. This view is consistent with increased temperature affording more **7a** and thus resulting in poorer regioselectivity. Conducting the reaction in a less polar solvent, such as benzene, results in a larger amount of **7a** being formed. While the S_NAr reaction with phosphine may be rate-limiting and a nonpolar solvent could stabilize an intermediate en route to **7a**, a full kinetic study would be required to confirm this.

Table 1. Ratio of 7a/7b for the Reaction of 1 with PPh_3 under Various Reaction Conditions[a]

solvent	T (°C)	7a/7b
C_6D_6	25	1:3
C_6D_6	60	1:2
$CDCl_3$	25	1:12
$CDCl_3$	60	1:5

[a]Trace amounts of the $Ph_3P{=}O$ adduct of **2** was observed by ^{31}P NMR spectroscopy after 48−96 hours. Ratios were determined by quantitative ^{31}P NMR spectroscopy.

CONCLUSIONS

The work described herein establishes the reactivity of boron-derived radicals with a series of nucleophiles, including tertiary and secondary phosphines $P(t\text{-}Bu)_3$, PPh_3, $HPPh_2$, and $HP(t\text{-}Bu)_2$, as well as IMes, DMAP, and quinuclidine, affording a unique and facile synthetic pathway to the zwitterionic products. The dominant regiochemistry of substitution observed for the tertiary phosphines, NHC, and quinuclidine-derived zwitterions is consistent with the nature of the LUMO and the steric demands of the nucleophile. In contrast, in the case of **9** and **10**, the observed isomers are thought to be favored by a hydrogen-bonding interaction of the secondary phosphine with the B-bound oxygen atoms. In the case of **15**, substitution occurs at the carbons α to oxygen. Although the resonance forms do suggest that these carbons are also electrophilic, it is presumably the comparatively small size of DMAP relative to the other nucleophiles used that allows it alone to access these α-carbons. Further studies of the utility of zwitterionic products derived from FLP generated radicals are the subject of ongoing work.

EXPERIMENTAL SECTION

General Considerations. All reactions and workup procedures were performed under an inert atmosphere of dry, oxygen-free N_2 using standard Schlenk techniques or a glovebox (MBraun, equipped with a −35 °C freezer) unless otherwise specified. Pentane, dichloromethane, and toluene (Aldrich) were dried using a Grubbs-type Innovative Technologies solvent purification system. Chloroform was dried by stirring over CaH_2 for several days followed by distillation. Deuterated solvents (CD_2Cl_2, $CDCl_3$, d_6-DMSO, d_8-THF) were purchased from Cambridge Isotope Laboratories, Inc., degassed, and stored over activated 4 Å molecular sieves prior to use, unless otherwise specified. DMAP, quinuclidine, and $PMes_3$ were purchased from Sigma-Aldrich. $P(t\text{-}Bu)_3$, PPh_3, $HP(t\text{-}Bu)_2$, $HPPh_2$, and IMes were purchased from Strem. All were used without further purification. Compounds **1** and **3** were prepared according to literature procedures.[45] Thin-layer chromatography (TLC) was performed on 0.5 mm EMD silica gel 60 F_{254} plates, with visualization of the developed plates under UV light (254 nm). Silica gel for glovebox manipulations was dried under vacuum at 150 °C. Column chromatography was performed with Silicycle Silia-P flash silica gel using plastic syringes (in an N_2-filled glovebox) or glass columns (in air).

NMR spectra were obtained on a Bruker Avance III 400 MHz, Agilent DD2 500 MHz, or Agilent DD2 600 MHz spectrometer, and spectra were referenced to residual solvent of CD_2Cl_2 (^1H = 5.32; ^{13}C = 54.0), $CDCl_3$ (^1H = 7.26; ^{13}C = 77.2), d_6-DMSO (^1H = 2.50; ^{13}C = 39.5), d_8-THF (^1H = 3.58 for OCH_2; ^{13}C = 67.6 for OCH_2), or externally (^{19}F, $CFCl_3$, ^{11}B, $(Et_2O)BF_3$, ^{31}P, 85% H_3PO_4). Chemical shifts (δ) are reported in ppm and coupling constants are listed in hertz. NMR assignments are supported by additional 2D experiments. Elemental analyses (C,H,N) and high resolution mass spectrometry (HRMS) were performed in house. UV−vis absorption spectra were obtained on a Agilent 8453 UV−vis spectrophotometer using dry dichloromethane or THF solutions in quartz cuvettes. Extinction coefficients were determined for the lowest energy absorbances in the visible region by successively diluting an initial stock solution prepared using volumetric glassware (3−4 mg of sample) and plotting absorbance vs concentration (in M) to determine the slope of the line.

Synthesis of 5. In a nitrogen-filled glovebox, $P(t\text{-}Bu)_3$ (30 mg, 0.15 mmol) was dissolved in 0.5 mL of THF and transferred to a 20 mL scintillation vial containing **1** (83 mg, 0.15 mmol). The $P(t\text{-}Bu)_3$ vial was rinsed with 2 × 0.5 mL of THF, and the washes were added to the reaction mixture. The scintillation vial was equipped with a magnetic stir bar, capped, and stirred at ambient glovebox temperature (35 °C) for 14 h. Over the course of the reaction, the solution changed from dark black yellow to a cloudy orange suspension. The volatiles were removed *in vacuo*, and the remaining material was triturated with pentane, followed by toluene, and finally CH_2Cl_2. NMR analysis of the 3 washes confirmed that the majority of **5** was in the CH_2Cl_2 wash. The material was removed from the glovebox, dry-packed onto Celite, and purified by flash column chromatography (100% CH_2Cl_2) on silica that had been pretreated with a 10% Et_3N in CH_2Cl_2 solution. One fraction was collected, which, upon concentration, was a bright yellow solid. This material contained a small amount of new phosphine impurities (as determined by NMR, which formed on the column); however these were easily removed by washing the yellow solid with excess toluene. After column chromatography and toluene washes, the desired product was isolated as a bright yellow solid in 66% yield (37 mg, 0.05 mmol).

^1H NMR (400 MHz, 298 K, CD_2Cl_2): δ 9.30 (dd, $^3J_{HP}$ = 11.4 Hz, $^4J_{HH}$ = 2.0 Hz, 1H, 4-C$\underline{H}$), 8.44 (d, $^3J_{HH}$ = 8.5 Hz, 1H, 8-C$\underline{H}$), 8.27 (dd, $^3J_{HH}$ = 8.9 Hz, $^4J_{HP}$ = 3.8 Hz, 1H, 1-C$\underline{H}$), 8.23−8.21 (m, 1H, 5-C$\underline{H}$), 7.91 (ddd, $^3J_{HH}$ = 8.9 Hz, $^3J_{HP}$ = 7.0 Hz, $^4J_{HH}$ = 2.0 Hz, 1H, 2-C$\underline{H}$), 7.65 (ddd, $^3J_{HH}$ = 8.1 Hz, $^3J_{HH}$ = 6.9 Hz, 1.0 Hz, 1H, 6-C$\underline{H}$), 7.53

DOI: 10.1021/jacs.6b11190
J. Am. Chem. Soc. 2017, 139, 426−435

(ddd, $^3J_{HH}$ = 8.4 Hz, $^3J_{HH}$ = 6.9 Hz, 1.4 Hz, 1H, 7-CH), 1.81 (d, $^3J_{HP}$ = 14.1 Hz, 27H, $PCMe_3$). ^{19}F NMR (377 MHz, 298 K, CD_2Cl_2): δ −136.0 (dd, $^3J_{FF}$ = 25 Hz, $^4J_{FF}$ = 10 Hz, 2F, *o*-C_6F_5), −161.2 (t, $^3J_{FF}$ = 20 Hz, 1F, *p*-C_6F_5), −165.9 to −166.1 (m, 2F, *m*-C_6F_5). $^{31}P\{^1H\}$ NMR (162 MHz, 298 K, CD_2Cl_2): δ 49.0. ^{11}B NMR (128 MHz, 298 K, CD_2Cl_2): δ 10.9. $^{13}C\{^1H\}$ NMR (101 MHz, 298 K, CD_2Cl_2), partial: δ 149.2 (s, 9-C), 142.7 (s, 10-C), 131.6 (d, $^2J_{CP}$ = 6 Hz, 4-CH), 128.6 (d, $^2J_{CP}$ = 6 Hz, 2-CH), 127.5 (s, 6-CH), 126.4 (br s, 11-C), 126.0 (s, 14-C), 125.5 (2, 13-C), 124.4 (s, 7-CH), 124.3 (d, $^3J_{CP}$ = 11 Hz, 12-C), 122.3 (s, 8-CH), 122.1 (s, 5-CH), 122.0 (d, $^3J_{CP}$ = 11 Hz, 1-CH), 105.8 (d, $^1J_{CP}$ = 67 Hz, 3-C), 41.8 (d, $^1J_{CP}$ = 30 Hz, $PCMe_3$), 32.1 (s, $PCMe_3$). HRMS (ESI) calcd for $[C_{38}H_{35}{}^{10}BF_{10}O_2P]^+$ ($[M + H]^+$) 754.2339, found 754.2325. Elemental analysis calcd (%) for $C_{38}H_{34}BF_{10}O_2P$: C 60.50; H 4.54. Found: C 59.99; H 4.54. $\lambda_{(abs)}$: 418 nm (CH_2Cl_2, ε = 2.1 × 10^4 M^{-1} cm^{-1}).

Synthesis of 7a and 7b. In a nitrogen-filled glovebox, PPh_3 (43 mg, 0.16 mmol) was weighed in a vial, dissolved in 1 mL of toluene, and the resulting solution was transferred to a vial containing boron radical **1** (150 mg, 0.27 mmol). The vial that contained the PPh_3 was rinsed with 2 × 1 mL toluene, and the washes were added to the reaction mixture. The resulting dark black solution was transferred to a 25 mL Schlenk bomb equipped with a magnetic stir bar. The vial that contained the reaction mixture was washed with 4 × 1 mL of toluene, making the total reaction volume 7 mL. The bomb was sealed, removed from the glovebox, and heated to 60 °C for 3 days. The reaction flask was then cooled to rt, and the volatiles were removed *in vacuo*. The residual orange-yellow precipitate was stirred over ∼10 mL of pentane. After decanting the pentane wash, the residual yellow-orange material was stirred over ∼5 mL of toluene. Finally, after decanting the toluene wash, the remaining yellow material was dissolved in CH_2Cl_2 and transferred into a vial. The toluene wash contained mostly **7a** with a small amount of **7b** and boronic ester **2**. The CH_2Cl_2 wash contained mostly **7b** with a small amount of **7a** and a very small amount of boronic ester **2**. The toluene wash was purified by flash column chromatography in the glovebox, using 1:1 pentane/CH_2Cl_2 as the eluent. Compound **7a** was isolated as an orange solid (28 mg, 0.03 mmol). The CH_2Cl_2 wash was purified by adding Et_2O to the impure material; a small amount of yellow solid did not dissolve in Et_2O, which was found to be pure **7b**. The Et_2O solution was left at ambient glovebox temperature (35 °C), and orange crystals grew from the solution. The mother liquor was decanted (which contained a mixture of **7a**, **7b**, and boronic ester **2**), and the crystals were found to be pure **7b**. The pure batches of **7b** were combined and concentrated to yield a yellow solid (75 mg, 0.09 mmol). In total, the 2 isomers were isolated in a combined yield of 93% (103 mg, 0.13 mmol). Single crystals of **7a** suitable for X-ray diffraction studies grew from an NMR scale reaction in $CDCl_3$ at room temperature. Single crystals of **7b** were grown from a saturated toluene solution of **7b** at −35 °C.

7b. ^1H NMR (400 MHz, 298 K, $CDCl_3$): δ 8.60 (dd, $^2J_{HP}$ = 15.8 Hz, $^4J_{HH}$ = 1.7 Hz, 1H, 4-CH), 8.41 (dd, $^3J_{HH}$ = 8.6 Hz, $^4J_{HP}$ = 4.1 Hz, 1H, 1-CH), 8.30 (d, $^3J_{HH}$ = 8.1 Hz, 1H, 8-CH), 8.02 (d, $^3J_{HH}$ = 8.4 Hz, 1H, 5-CH), 7.88 (t, $^3J_{HH}$ = 7.3 Hz, 3H, Ph *para*-CH), 7.75−7.64 (m, 12H, Ph *ortho*-CH and *para*-CH), 7.55−7.51 (m, 1H, 7-CH), 7.39 (ddd, $^3J_{HP}$ = 10.6 Hz, $^3J_{HH}$ = 8.6 Hz, $^4J_{HH}$ = 1.7 Hz, 1H, 2-CH), 7.34−7.30 (m, 1H, 6-CH). ^{19}F NMR (377 MHz, 298 K, $CDCl_3$): δ −135.2 (dd, $^3J_{FF}$ = 25.4 Hz, $^4J_{FF}$ = 9.6 Hz, 2F, *o*-C_6F_5), −160.6 (t, $^3J_{FF}$ = 20.4 Hz, 1F, *p*-C_6F_5), −165.4 to −165.5 (m, 2F, *m*-C_6F_5). $^{31}P\{^1H\}$ NMR (162 MHz, 298 K, $CDCl_3$): δ 23.7 (s). ^{11}B NMR (128 MHz, 298 K, $CDCl_3$): δ 11.1 (s). $^{13}C\{^1H\}$ NMR (126 MHz, 298 K, $CDCl_3$), partial: δ 150.2 (s, C9), 148.4 (dm, $^1J_{CF}$ ∼ 243 Hz, C_6F_5), 142.8 (s, C10), 139.5 (dm, $^1J_{CF}$ ∼ 248 Hz, C_6F_5), 137.0 (dm, $^1J_{CF}$ ∼ 249 Hz, C_6F_5), 135.4 (d, $^4J_{CP}$ = 3 Hz, *p*-Ph), 134.4 (d, $^2J_{CP}$ = 10 Hz, *o*-Ph), 131.4 (d, $^2J_{CP}$ = 12 Hz, CH-4), 130.6 (d, $^3J_{CP}$ = 13 Hz, *m*-Ph), 127.0 (br s, CH-7 and C11), 126.7 (d, $^2J_{CP}$ = 11 Hz, CH-2), 125.4 (s, C13), 125.1 (br s, C14), 124.2 (d, $^3J_{CP}$ = 14 Hz, C12), 124.0 (s, CH-6), 123.0 (d, $^3J_{CP}$ = 14 Hz, CH-1), 122.1 (s, CH-5), 121.7 (s, CH-8), 119.5 (d, $^1J_{CP}$ = 90 Hz, *i*-Ph), 103.0 (d, $^1J_{CP}$ = 97 Hz, C3). HRMS (ESI) calcd for $[C_{44}H_{23}BF_{10}O_2P]^+$ ($[M + H]^+$) 815.1371, found 815.1384. Elemental analysis calcd (%) for $C_{44}H_{22}BF_{10}O_2P$: C 64.89; H 2.72. Found: C 63.97; H 2.68. Elemental analysis was consistently low on % carbon. $\lambda_{(abs)}$: 431 nm (CH_2Cl_2, ε = 2.4 × 10^4 M^{-1} cm^{-1}).

7a. ^1H NMR (400 MHz, 298 K, d_8-THF): δ 9.24 (d, $^3J_{HH}$ = 8.3 Hz, 1H, 4-CH), 8.81 (d, $^3J_{HH}$ = 8.4 Hz, 1H, 8-CH), 8.15 (d, $^3J_{HH}$ = 7.6 Hz, 1H, 5-CH), 7.99−6.98 (br, 15 Hz, PPh_3), 7.61−7.57 (m, 1H, 6-CH), 7.53−7.49 (m, 1H, 7-CH), 7.38−7.33 (m, 1H, 3-CH), 7.22 (dd, $^3J_{HH}$ = 7.4 Hz, $^3J_{HP}$ = 17.2 Hz, 1H, 2-CH). ^{19}F NMR (377 MHz, 298 K, d_8-THF): δ −134.3 (dd, $^3J_{FF}$ = 26 Hz, $^4J_{FF}$ = 9 Hz, 2F, *o*-C_6F_5), −163.5 (t, $^3J_{FF}$ = 20 Hz, 1F, *p*-C_6F_5), −167.2 to −167.3 (m, 2F, *m*-C_6F_5). $^{31}P\{^1H\}$ NMR (162 MHz, 298 K, d_8-THF): δ 29.0 (s). ^{11}B NMR (128 MHz, 298 K, d_8-THF): δ 10.0 (s). $^{13}C\{^1H\}$ NMR (126 MHz, 298 K, d_8-THF), partial: δ 149.6 (s, C9), 149.0 (dm, $^1J_{CF}$ ∼ 241 Hz, C_6F_5), 141.3 (s, C10), 140.1 (dm, $^1J_{CF}$ ∼ 246 Hz, C_6F_5), 138.7 (d, $^2J_{CP}$ = 11 Hz, CH-2), 137.3 (dm, $^1J_{CF}$ ∼ 241 Hz, C_6F_5), 134.2 (br, PPh_3), 132.2 (s, CH-4), 129.7 (br, PPh_3), 127.6 (s, CH-7), 127.3 (s, C13), 126.8 (d, $^3J_{CP}$ = 10 Hz, C12), 126.2 (d, $^2J_{CP}$ = 6 Hz, C11), 125.5 (s, C14), 125.1 (br, PPh_3), 124.8 (s, CH-6), 124.3 (br, PPh_3), 124.1 (s, CH-5), 122.2 (s, CH-8), 120.8 (d, $^3J_{CP}$ = 15 Hz, CH-3), 106.3 (d, $^1J_{CP}$ = 91 Hz, C1). HRMS (DART) calcd for $[C_{44}H_{23}BF_{10}O_2P]^+$ ($[M + H]^+$) 815.1369, found 815.1373. Elemental analysis calcd (%) for $C_{44}H_{22}BF_{10}O_2P$: C 64.89; H 2.72. Found: C 64.50; H 2.89. $\lambda_{(abs)}$: 401 nm (CH_2Cl_2, ε = 9 × 10^3 M^{-1} cm^{-1}), 470 nm (CH_2Cl_2, ε = 4 × 10^3 M^{-1} cm^{-1}).

Synthesis of 8a and 8b. In a nitrogen-filled glovebox, PPh_3 (13 mg, 0.05 mmol) was weighed in a vial and dissolved in 0.5 mL of $CHCl_3$, and the resulting solution was transferred to a vial containing boron radical **3** (58 mg, 0.1 mmol). The vial that contained the PPh_3 was rinsed with 2 × 0.5 mL of $CHCl_3$, and the washes were added to the reaction mixture. The resulting dark black solution was transferred to a 25 mL Schlenk bomb equipped with a magnetic stir bar. The vial that contained the reaction mixture was washed with 2 × 0.5 mL $CHCl_3$, making the total reaction volume 2.5 mL. The bomb was sealed, removed from the glovebox, and heated to 65 °C for 36 h. The reaction flask was then cooled to rt, and the volatiles were removed *in vacuo*. The residual pink precipitate was dissolved in CH_2Cl_2 and filtered into a tared vial. The solution was concentrated *in vacuo*, and the dried material was stirred over ∼6 mL of pentane. The pentane was decanted, and the remaining material (crude yield 47 mg) was purified by pTLC in air, using 30:70 hexanes/CH_2Cl_2 as the eluent. Two bands were isolated, the less polar being **8a** (17 mg), which is an orange-pink solid, and the more polar being **8b** (15 mg), which is a deep pink color. In total, the 2 isomers were isolated in a combined yield of 76% (32 mg, 0.04 mmol). Single crystals of **8a** suitable for X-ray diffraction studies grew from an NMR scale reaction in $CDCl_3$ at room temperature. Single crystals of **8b** were grown by slow diffusion of pentane into a CH_2Cl_2 solution of **8b** at −35 °C.

8b. ^1H NMR (500 MHz, 298 K, $CDCl_3$): δ 8.79 (dd, $^3J_{HH}$ = 7.0 Hz, $^4J_{HH}$ = 1.5 Hz, 1H, 6-CH), 8.42 (dd, $^3J_{HH}$ = 8.5 Hz, $^4J_{HP}$ = 3.0 Hz, 1H, 3-CH), 8.07−8.02 (m, 2H, 7-CH and 8-CH), 7.88 (d, $^3J_{HH}$ = 9.0 Hz, 1H, 9-CH), 7.77−7.72 (m, 3H, *para*-CH), 7.63−7.59 (m, 12H, *ortho* and *meta*-CH), 7.46 (d, $^3J_{HH}$ = 9.0 Hz, 1H, 10-CH), 7.42 (dd, $^3J_{HP}$ = 15.0 Hz, $^3J_{HH}$ = 8.5 Hz, 1H, 2-CH). ^{19}F NMR (377 MHz, 298 K, $CDCl_3$): δ −135.1 (dd, $^3J_{FF}$ = 24.9 Hz, $^4J_{FF}$ = 10.2 Hz, 2F, *o*-C_6F_5), −160.5 (t, $^3J_{FF}$ = 20.2 Hz, 1F, *p*-C_6F_5), −165.3 to −165.5 (m, 2F, *m*-C_6F_5). $^{31}P\{^1H\}$ NMR (162 MHz, 298 K, $CDCl_3$): δ 22.3 (s). ^{11}B NMR (128 MHz, 298 K, $CDCl_3$): δ 11.4 (s, borate). $^{13}C\{^1H\}$ NMR (126 MHz, 298 K, $CDCl_3$), partial: δ 150.2 (s, C5), 148.2 (dm, $^1J_{CF}$ ∼ 244 Hz, C_6F_5), 143.7 (s, C4), 139.3 (dm, $^1J_{CF}$ ∼ 241 Hz, C_6F_5), 136.7 (dm, $^1J_{CF}$ ∼ 249 Hz, C_6F_5), 134.8 (d, $^4J_{CP}$ = 3.0 Hz, *p*-Ph), 134.7 (d, $^2J_{CP}$ = 8.8 Hz, C14), 134.1 (d, $^2J_{CP}$ = 10.2 Hz, *o*-Ph), 131.4 (d, $^2J_{CP}$ = 12.2 Hz, C2), 130.7 (s, C9), 130.3 (d, $^3J_{CP}$ = 12.7 Hz, *m*-Ph), 129.5 (s, C13), 128.1 (d, $^4J_{CP}$ = 2.5 Hz, C11), 126.3 (s, C7), 125.0 (s, C8), 124.0 (d, $^3J_{CP}$ = 8.2 Hz, C10), 123.2 (d, $^5J_{CP}$ = 1.4 Hz, C12), 122.2 (br s, C6), 120.3 (d, $^1J_{CP}$ = 88.6 Hz, *i*-Ph), 120.0 (d, $^3J_{CP}$ = 11.2 Hz, C15), 118.6 (d, $^4J_{CP}$ = 1.6 Hz, C16), 117.2 (d, $^3J_{CP}$ = 14.7 Hz, C3), 96.5 (d, $^1J_{CP}$ = 91.6 Hz, C1). HRMS (DART) calcd for $[C_{46}H_{23}BF_{10}O_2P]^+$ ($[M + H]^+$) 839.1369, found 839.1383. Elemental analysis calcd (%) for $C_{46}H_{22}BF_{10}O_2P$: C 65.90; H 2.64. Found: C 65.96; H 3.00. $\lambda_{(abs)}$: 436 nm (CH_2Cl_2, ε = 5 × 10^3 M^{-1} cm^{-1}), 515 nm (CH_2Cl_2, ε = 1.4 × 10^4 M^{-1} cm^{-1}).

DOI: 10.1021/jacs.6b11190
J. Am. Chem. Soc. 2017, 139, 426−435

8a. ^{1}H NMR (500 MHz, 298 K, $CDCl_3$): δ 8.71 (dd, $^{3}J_{HH}$ = 7.8 Hz, $^{4}J_{HH}$ = 0.8 Hz, 1H, 6-C<u>H</u>), 8.31 (d, $^{3}J_{HH}$ = 9.0 Hz, 1H, 9-C<u>H</u>), 8.23 (d, $^{3}J_{HH}$ = 7.5 Hz, 1H, 8-C<u>H</u>), 8.13 (t, $^{3}J_{HH}$ = 7.8 Hz, 1H, 7-C<u>H</u>), 8.04 (d, $^{3}J_{HH}$ = 9.0 Hz, 1H, 10-C<u>H</u>), 7.77 (dd, $^{3}J_{HH}$ = 8.2 Hz, $^{4}J_{HP}$ = 2.8 Hz, 1H, 1-C<u>H</u>), 7.36 (dd, $^{3}J_{HP}$ = 16.0 Hz, $^{3}J_{HH}$ = 8.0 Hz, 1H, 2-C<u>H</u>), 7.89–7.19 (br, 15 H, 3xPh). ^{19}F NMR (377 MHz, 298 K, $CDCl_3$): δ −134.1 (dd, $^{3}J_{FF}$ = 25.8 Hz, $^{4}J_{FF}$ = 9.2 Hz, 2F, *o*-C_6F_5), −160.9 (t, $^{3}J_{FF}$ = 20.4 Hz, 1F, *p*-C_6F_5), −165.3 to −165.4 (m, 2F, *m*-C_6F_5). ^{31}P{^{1}H} NMR (162 MHz, 298 K, $CDCl_3$): δ 28.6 (s). ^{11}B NMR (128 MHz, 298 K, $CDCl_3$): δ 10.2 (br s). ^{13}C{^{1}H} NMR (126 MHz, 298 K, $CDCl_3$), partial: δ 149.4 (s, C5), 147.9 (dm, $^{1}J_{CF}$ ∼ 242 Hz, C_6F_5), 141.5 (d, $^{3}J_{CP}$ = 3.9 Hz, C4), 139.1 (dm, $^{1}J_{CF}$ ∼ 240 Hz, C_6F_5), 136.8 (d, $^{4}J_{CP}$ = 2.9 Hz, C14), 136.2 (dm, $^{1}J_{CP}$ ∼ 248 Hz, C_6F_5), 133.6 (d, $^{2}J_{CP}$ = 11.2 Hz, C2), 133.0 (br s, *o*- and *p*-Ph), 132.2 (s, C9), 131.2 (d, $^{5}J_{CP}$ = 1.4 Hz, C13), 128.6 (br s, *m*-Ph), 126.6 (d, $^{5}J_{CP}$ = 1.5 Hz, C10), 126.4 (d, $^{2}J_{CP}$ = 7.3 Hz, C11), 126.3 (s, C7), 125.0 (s, C8), 122.5 (s, C12), 121.3 (s, C6), 119.6 (d, $^{3}J_{CP}$ = 11.2 Hz, C15), 119.1 (d, $^{3}J_{CP}$ = 15.0 Hz, C1), 119.0 (d, $^{4}J_{CP}$ = 1.3 Hz, C16), 97.8 (d, $^{1}J_{CP}$ = 94.4 Hz, C3). HRMS (DART) calcd for $[C_{46}H_{23}BF_{10}O_2P]^+$ ($[M + H]^+$) 839.1369, found 839.1360. Elemental analysis calcd (%) for $C_{46}H_{22}BF_{10}O_2P$: C 65.90; H 2.64. Found: C 65.50; H 2.85. $\lambda_{(abs)}$: 426 nm (CH_2Cl_2, ε = 5 × 10^3 M^{-1} cm^{-1}), 500 nm (CH_2Cl_2, ε = 1.1 × 10^4 M^{-1} cm^{-1}).

Synthesis of 9. In a nitrogen-filled glovebox, $HPPh_2$ (14 mg, 0.08 mmol) was weighed in a vial and dissolved in 1 mL of toluene, and the resulting solution was transferred to a vial containing boron radical **3** (87 mg, 0.15 mmol). The vial that contained the $HPPh_2$ was rinsed with 2 × 1 mL of toluene, and the washes were added to the reaction mixture. An additional 4 mL of toluene was added to the reaction mixture, making the total reaction volume 7 mL. A magnetic stir bar was added to the vial, which was capped and stirred at ambient glovebox temperature (35 °C) for 5 days. The volatiles were then removed *in vacuo*. The residual pink and white precipitates were stirred over ∼10 mL of pentane. After decanting the pentane wash, the residual materials were stirred over ∼5 mL of toluene. Finally, after decanting the toluene wash, the remaining material was dissolved in CH_2Cl_2, filtered through a plug of silica, and transferred into a vial. The toluene and CH_2Cl_2 washes were concentrated *in vacuo*; the CH_2Cl_2 wash contained pure **9** (22 mg) as a deep pink solid, and the toluene wash was purified by flash column chromatography (in air) using 1:1 CH_2Cl_2/pentane as the eluent, isolating an additional 22 mg of **9**. In total, **9** was isolated in 77% yield (44 mg, 0.06 mmol). Single crystals were grown from by slow diffusion of pentane into a CH_2Cl_2 solution of **9** at −35 °C.

^{1}H NMR (400 MHz, 298 K, $CDCl_3$): δ 9.87 (d, $^{1}J_{HP}$ = 549.2 Hz, 1H, P<u>H</u>), 8.75 (d, $^{3}J_{HH}$ = 8.0 Hz, 1H, 6-C<u>H</u>), 8.30 (d, $^{3}J_{HH}$ = 8.8 Hz, 1H, 9-C<u>H</u>), 8.22 (d, $^{3}J_{HH}$ = 7.6 Hz, 1H, 8-C<u>H</u>), 8.13 (t, $^{3}J_{HH}$ = 7.6 Hz, 1H, 7-C<u>H</u>), 8.03 (d, $^{3}J_{HH}$ = 8.8 Hz, 1H, 10-C<u>H</u>), 7.81 (dd, $^{3}J_{HH}$ = 8.2 Hz, $^{4}J_{HP}$ = 3.0 Hz, 1H, 1-C<u>H</u>), 7.71–7.66 (m, 2H, PPh_2), 7.61–7.51 (m, 8H, PPh_2), 7.42 (dd, $^{3}J_{HP}$ = 15.8 Hz, $^{3}J_{HH}$ = 8.0 Hz, 1H, 2-C<u>H</u>). ^{19}F NMR (377 MHz, 298 K, $CDCl_3$): δ −135.5 (d, $^{3}J_{FF}$ = 24 Hz, 2F, *o*-C_6F_5), −160.1 (t, $^{3}J_{FF}$ = 20 Hz, 1F, *p*-C_6F_5), −164.7 to −164.9 (m, 2F, *m*-C_6F_5). ^{31}P{^{1}H} NMR (162 MHz, 298 K, $CDCl_3$): δ 6.25 (s). ^{31}P NMR (162 MHz, 298 K, $CDCl_3$): δ 6.26 (d, $^{1}J_{PH}$ = 547 Hz, P<u>H</u>). ^{11}B NMR (128 MHz, 298 K, $CDCl_3$): δ 10.7 (s). ^{13}C{^{1}H} NMR (126 MHz, 298 K, $CDCl_3$), partial: δ 149.1 (s, C5), 147.9 (dm, $^{1}J_{CF}$ ∼ 243 Hz, C_6F_5), 142.0 (d, $^{3}J_{CP}$ = 3 Hz, C4), 139.5 (dm, $^{1}J_{CF}$ ∼ 248 Hz, C_6F_5), 137.1 (d, $^{4}J_{CP}$ = 3 Hz, C11), 136.8 (dm, $^{1}J_{CF}$ ∼ 250 Hz, C_6F_5), 134.4 (d, $^{4}J_{CP}$ = 3 Hz, *p*-Ph), 133.5 (d, $^{2}J_{CP}$ = 11 Hz, *o*-Ph), 132.7 (s, C9), 131.6 (d, $^{2}J_{CP}$ = 11 Hz, C2), 131.3 (d, $^{5}J_{CP}$ = 1 Hz, C14), 130.0 (d, $^{3}J_{CP}$ = 13 Hz, *m*-Ph), 126.7 (s, C7), 126.5 (d, $^{5}J_{CP}$ = 1 Hz, C10), 126.2 (d, $^{2}J_{CP}$ = 8 Hz, C15), 125.5 (s, C8), 123.0 (s, C16), 121.9 (s, C6), 119.8 (d, $^{3}J_{CP}$ = 15 Hz, C1), 119.5 (d, $^{1}J_{CP}$ = 91 Hz, *i*-Ph), 119.3 (d, $^{3}J_{CP}$ = 11 Hz, C12), 119.1 (d, $^{4}J_{CP}$ = 1 Hz, C13), 95.3 (d, $^{1}J_{CP}$ = 93 Hz, C3). HRMS (DART) calcd for $[C_{40}H_{19}BF_{10}O_2P]^+$ ($[M + H]^+$) 763.1056, found 763.1049. Elemental analysis calcd (%) for $C_{40}H_{18}BF_{10}O_2P$: C 63.02; H 2.38. Found: C 62.79; H 2.33. $\lambda_{(abs)}$: 427 nm (CH_2Cl_2, ε = 5 × 10^3 M^{-1} cm^{-1}), 498 nm (CH_2Cl_2, ε = 1.1 × 10^4 M^{-1} cm^{-1}).

Synthesis of 10. In a nitrogen-filled glovebox, HP(*t*-Bu)$_2$ (13 mg, 0.09 mmol) was dissolved in 1 mL of toluene and transferred to a scintillation vial equipped with a magnetic stir bar containing **3** (100 mg, 0.17 mmol). The phosphine vial was rinsed with 2 × 1 mL of toluene, and the washes were added to the reaction mixture. An additional 4 mL of toluene was used to dilute the reaction mixture, making the total volume 7 mL. The mixture was stirred for 2 days at ambient glovebox temperature (35 °C). Over the course of the reaction, the solution changed from dark blue-black to cloudy orange. Upon completion, the volatiles were removed *in vacuo*. The remaining residue was washed with ∼10 mL of pentane. The material was purified by flash column chromatography (1:1 CH_2Cl_2/pentane) in an N_2-filled glovebox. The fractions were concentrated to yield **10** as an orange solid in 69% yield (43 mg, 0.06 mmol). Crystals suitable for X-ray diffraction studies were grown by slow evaporation of a CH_2Cl_2 solution of **10**.

^{1}H NMR (600 MHz, 298 K, $CDCl_3$): δ 9.48 (d, $^{1}J_{HP}$ = 508.2 Hz, 1H, P<u>H</u>), 8.82 (dd, $^{3}J_{HH}$ = 7.8 Hz, $^{4}J_{HH}$ = 1.2 Hz, 1H, C<u>H</u>-6), 8.28 (d, $^{3}J_{HH}$ = 8.7 Hz, 1H, C<u>H</u>-9), 8.21 (d, $^{3}J_{HH}$ = 7.8 Hz, $^{4}J_{HH}$ = 1.2 Hz, 1H, C<u>H</u>-8), 8.14 (t, $^{3}J_{HH}$ = 7.8 Hz, 1H, C<u>H</u>-7), 8.04 (d, $^{3}J_{HH}$ = 8.7 Hz, 1H, C<u>H</u>-10), 7.99 (dd, $^{3}J_{PH}$ = 11.4 Hz, $^{3}J_{HH}$ = 8.1 Hz, 1H, C<u>H</u>-2), 7.95 (dd, $^{3}J_{HH}$ = 8.1 Hz, $^{4}J_{PH}$ = 2.6 Hz, 1H, C<u>H</u>-1), 1.56 (d, $^{3}J_{PH}$ = 16.4 Hz, 18H, *t*-Bu). ^{19}F NMR (377 MHz, 298 K, $CDCl_3$): δ −135.9 (dd, $^{3}J_{FF}$ = 21 Hz, $^{4}J_{FF}$ = 6 Hz, 2F, *o*-C_6F_5), −159.8 (t, $^{3}J_{FF}$ = 20 Hz, 1F, *p*-C_6F_5), −164.7 to −164.9 (m, 2F, *m*-C_6F_5). ^{31}P{^{1}H} NMR (162 MHz, 298 K, $CDCl_3$): δ 27.7 (s). ^{31}P NMR (162 MHz, 298 K, $CDCl_3$): δ 27.7 (d, $^{1}J_{PH}$ = 508 Hz). ^{11}B NMR (128 MHz, 298 K, $CDCl_3$): 10.6 (s). ^{13}C{^{1}H} NMR (126 MHz, 298 K, $CDCl_3$), partial: δ 149.3 (s, C5), 147.9 (dm, $^{1}J_{CF}$ ∼ 241 Hz, C_6F_5), 141.1 (d, $^{3}J_{CP}$ = 2 Hz, C4), 139.6 (dm, $^{1}J_{CF}$ ∼ 248 Hz, C_6F_5), 137.1 (dm, $^{1}J_{CF}$ ∼ 244 Hz, C_6F_5), 136.0 (d, $^{4}J_{CP}$ = 3 Hz, C11), 131.9 (s, C9), 131.2 (d, $^{5}J_{CP}$ = 1 Hz, C14), 128.8 (d, $^{2}J_{CP}$ = 6 Hz, C2), 126.8 (d, $^{2}J_{CP}$ = 3 Hz, C15), 126.69 (s, C10), 126.68 (s, C7), 125.3 (s, C8), 123.1 (s, C16), 121.7 (s, C6), 120.4 (d, $^{3}J_{CP}$ = 10 Hz, C12), 119.6 (d, $^{3}J_{CP}$ = 13 Hz, C1), 119.3 (d, $^{4}J_{CP}$ = 1 Hz, C13), 99.5 (d, $^{1}J_{CP}$ = 73 Hz, C3), 35.4 (d, $^{1}J_{CP}$ = 36 Hz, <u>C</u>(CH_3)$_3$), 28.5 (d, $^{3}J_{CP}$ = 2 Hz, C(<u>C</u>H$_3$)$_3$). HRMS (DART) calcd for $[C_{36}H_{27}BF_{10}O_2P]^+$ ($[M + H]^+$) 723.1682, found 723.1679. Elemental analysis calcd (%) for $C_{36}H_{26}BF_{10}O_2P$: C 59.86; H 3.63. Found: C 59.16; H 3.59. Elemental analysis was consistently low on % carbon. $\lambda_{(abs)}$: 423 nm (CH_2Cl_2, ε = 5 × 10^3 M^{-1} cm^{-1}), 482 nm (CH_2Cl_2, ε = 8 × 10^3 M^{-1} cm^{-1}).

Synthesis of 11. In a nitrogen-filled glovebox, IMes (46 mg, 0.15 mmol) was dissolved in 0.5 mL of THF and transferred dropwise to a 20 mL scintillation vial containing a solution of **1** (83 mg, 0.15 mmol) in 0.5 mL of THF. The IMes vial was rinsed with 0.5 mL of THF, and the wash was added to the reaction mixture. The solution immediately changed from dark black yellow to clear orange-red. The volatiles were removed immediately *in vacuo*, and the remaining material was triturated with pentane, followed by toluene, Et_2O, and finally THF. The material from the THF wash was removed from the glovebox, dry-packed onto Celite, and purified by flash column chromatography (100% CH_2Cl_2) on silica that had been pretreated with a 10% Et_3N in CH_2Cl_2 solution. One fraction was collected, and **11** was isolated as a bright yellow solid in 68% yield (44 mg, 0.05 mmol).

^{1}H NMR (400 MHz, 298 K, d_8-THF): δ 8.19 (d, $^{4}J_{HH}$ = 1.9 Hz, 1H, 4-C<u>H</u>), 8.08 (dd, $^{3}J_{HH}$ = 8.2 Hz, $^{4}J_{HH}$ = 1.3 Hz, 1H, 8-C<u>H</u>), 8.05 (s, 2H, imidazole C<u>H</u>), 7.80 (d, $^{3}J_{HH}$ = 8.7 Hz, 1H, 1-C<u>H</u>), 7.79 (d, $^{3}J_{HH}$ = 8.5 Hz, 1H, 5-C<u>H</u>), 7.43 (ddd, $^{3}J_{HH}$ = 8.0 Hz, 6.9 Hz, $^{4}J_{HH}$ = 1.0 Hz, 1H, 7-C<u>H</u>), 7.25 (ddd, $^{3}J_{HH}$ = 8.4 Hz, 6.9 Hz, $^{4}J_{HH}$ = 1.4 Hz, 1H, 6-C<u>H</u>), 7.14 (d, $^{4}J_{HH}$ = 0.4 Hz, 4H, Mes C<u>H</u>), 6.92 (dd, $^{3}J_{HH}$ = 8.7 Hz, $^{4}J_{HH}$ = 1.9 Hz, 1H, 2-C<u>H</u>), 2.29 (s, 6H, Mes *p*-CH_3), 2.17 (s, 12H, Mes *o*-CH_3). ^{19}F NMR (377 MHz, 298 K, d_8-THF): δ −135.4 to −135.5 (m, 2F, *o*-C_6F_5), −163.7 (t, $^{3}J_{FF}$ = 20 Hz, 1F, *p*-C_6F_5), −167.8 to −168.0 (m, 2F, *m*-C_6F_5). ^{11}B NMR (128 MHz, 298 K, d_8-THF): δ 10.6 (s, borate). ^{13}C{^{1}H} NMR (126 MHz, 298 K, d_8-THF), partial: δ 149.5 (s, C9), 147.4 (s, imidazole *q*-<u>C</u>), 143.7 (s, C10), 142.7 (s, Mes *o*-<u>C</u>), 135.5 (s, Mes *p*-<u>C</u>), 132.7 (s, Mes *i*-<u>C</u>), 131.3 (s, Mes *m*-<u>C</u>H), 127.0 (s, C7), 126.39 (s, C11), 126.37 (s, C13), 126.0 (s, C14), 125.9 (s, C4), 125.4 (s, imidazole <u>C</u>H), 124.3 (C12), 123.7 (s, C6), 123.2 (s,

DOI: 10.1021/jacs.6b11190
J. Am. Chem. Soc. 2017, 139, 426–435

C2), 122.7 (s, C5), 122.4 (s, C8), 122.3 (s, C1), 111.9 (s, C3), 21.1 (s, Mes *p*-CH_3), 17.9 (s, Mes *o*-CH_3). HRMS (ESI) calcd for $[C_{47}H_{32}{}^{10}BF_{10}N_2O_2]^+$ ($[M + H]^+$) 856.2428, found 856.2396. Satisfactory elemental analysis could not be obtained after several attempts. $\lambda_{(abs)}$: 458 nm (CH_2Cl_2, $\varepsilon = 1.4 \times 10^4$ M^{-1} cm^{-1}).

Synthesis of 13 and 14. In a nitrogen-filled glovebox, radical **1** (80 mg, 0.14 mmol) was weighed in a 20 mL scintillation vial equipped with a magnetic stir bar. Two milliliters of toluene was added to **1**, forming a dark black-yellow solution. Quinuclidine (24 mg, 0.22 mmol) was transferred to the solution of **1** in 3 × 0.5 mL of toluene, making the final reaction volume 3.5 mL. The vial was capped and vigorously stirred at ambient glovebox temperature (35 °C) for 1 h, during which time the solution becomes cloudy and turns a yellow-brown color. The volatiles were then removed *in vacuo* to reveal a yellow solid. The material was stirred over 2 × 5 mL of CH_2Cl_2, collecting the wash in a separate vial. The residual material was dissolved in MeCN and filtered. Both washes were concentrated *in vacuo*. The MeCN wash was found to contain pure **13** in 93% yield (45 mg, 0.07 mmol). The CH_2Cl_2 wash contained quinuclidine-ligated **2** and a small amount of HC_6F_5, suggesting that the [quin$_2$H][borate] salt decomposed in solution. Single crystals of **13** were grown by vapor diffusion of hexanes into a THF solution of **13** at rt. Single crystals of **14** were grown in an NMR scale reaction of **1** with quinuclidine in d_8-toluene.

^{1}H NMR (400 MHz, 298 K, d_8-THF): δ 8.83 (d, $^4J_{HH}$ = 2.8 Hz, 1H, C<u>H</u>-4), 8.61 (d, $^3J_{HH}$ = 8.4 Hz, 1H, C<u>H</u>-5), 8.21 (d, $^3J_{HH}$ = 9.2 Hz, 1H, C<u>H</u>-1), 8.18−8.16 (m, 1H, C<u>H</u>-8), 7.74 (dd, $^3J_{HH}$ = 9.2 Hz, $^4J_{HH}$ = 2.8 Hz, 1H, C<u>H</u>-2), 7.54−7.49 (m, 1H, C<u>H</u>-7), 7.36 (ddd, $^3J_{HH}$ = 8.4 Hz, 6.8 Hz, $^4J_{HH}$ = 1.3 Hz, 1H, C<u>H</u>-6), 4.11−4.03 (m, 6H, N−C<u>H$_2$</u>), 2.31−2.26 (m, 1H, quin C<u>H</u>), 2.24−2.15 (m, 6H, N−CH$_2$−C<u>H$_2$</u>). ^{19}F NMR (377 MHz, 298 K, d_8-THF): δ −135.2 to −135.3 (m, 2F, *o*-C_6F_5), −163.7 (t, $^3J_{FF}$ = 20 Hz, 1F, *p*-C_6F_5), −167.7 to −167.9 (m, 2F, *m*-C_6F_5). ^{11}B NMR (128 MHz, 298 K, d_8-THF): δ 11.1 (s). ^{13}C{^{1}H} NMR (126 MHz, 298 K, d_8-THF), partial: δ 149.1 (dm, $^1J_{CF}$ ∼ 244 Hz, C_6F_5), 147.3 (s, C9), 143.6 (s, C10), 140.6 (s, C3), 127.1 (s, C7), 126.6 (s, C14), 126.1 (C13), 125.3 (s, C11), 124.8 (s, C12), 123.6 (s, C1), 123.3 (s, C5), 123.1 (s, C6), 122.4 (s, C8), 117.1 (s, C2), 115.6 (C4), 59.6 (s, N-<u>C</u>H$_2$), 21.0 (s, quin <u>C</u>H). *N*−*CH$_2$*-*<u>C</u>H$_2$* ^{13}C resonance overlaps with solvent peak (see SI Figure 54). HRMS (DART) calcd for $[C_{33}H_{21}BF_{10}NO_2]^+$ ($[M + H]^+$) 664.1506, found 664.1515. Elemental analysis calcd (%) for $C_{33}H_{20}BF_{10}NO_2$: C 59.75; H 3.04; N 2.11. Found: C 58.36; H 3.08; N 1.94. Elemental analysis was consistently low on % carbon. $\lambda_{(abs)}$: 445 nm (THF, $\varepsilon = 2 \times 10^3$ M^{-1} cm^{-1}), 468 nm (THF, $\varepsilon = 2 \times 10^3$ M^{-1} cm^{-1}).

Synthesis of 15. In a nitrogen-filled glovebox, radical **1** (55 mg, 0.10 mmol) was weighed in a 20 mL scintillation vial equipped with a magnetic stir bar. Two milliliters of toluene was added to the radical, which resulted in a very dark black-yellow solution. DMAP (12 mg, 0.10 mmol) was weighed and transferred to the solution of **1** using 3 × 0.5 mL of toluene. An additional 1.5 mL of toluene was added to the reaction mixture. The homogeneous solution was stirred at room temperature for 48 h, during which time the reaction mixture became an orange solution with a yellow-orange precipitate. The volatiles were removed *in vacuo* revealing a yellow precipitate. Pentane (∼5 mL) was added to the precipitate, which produced a suspension that was filtered through a frit. The precipitate was washed thoroughly with pentane, collected off the frit, and dried *in vacuo*. This yielded the desired product as a bright yellow solid in quantitative yield (67 mg, 0.05 mmol). Single crystals suitable for X-ray diffraction studies were grown from a saturated CH_2Cl_2 solution of **15** at −35 °C.

^{1}H NMR (400 MHz, 298 K, d_6-DMSO): δ 8.68 (d, $^3J_{HH}$ = 8.4 Hz, 2H, anion 4/5-C<u>H</u>), 8.24 (d, $^3J_{HH}$ = 8.1 Hz, 2H, cation 4/5-C<u>H</u>), 8.09 (dd, $^3J_{HH}$ = 8.0 Hz, $^4J_{HH}$ = 2.1 Hz, 2H, cation DMAP *o*-C<u>H</u>), 7.90 (dd, $^3J_{HH}$ = 8.1 Hz, $^4J_{HH}$ = 1.4 Hz, 2H, anion 1/8-C<u>H</u>), 7.56−7.48 (m, 4H, cation 3/6-C<u>H</u> and anion 2/7-C<u>H</u>), 7.36 (ddd, $^3J_{HH}$ = 8.4, 6.8 Hz, $^4J_{HH}$ = 1.5 Hz, 2H, anion 3/6-C<u>H</u>), 7.30−7.26 (m, 2H, cation 2/7-C<u>H</u>), 7.12 (dd, $^3J_{HH}$ = 7.9 Hz, $^4J_{HH}$ = 2.2 Hz, 2H, cation DMAP *o*-C<u>H</u>), 7.09−7.03 (m, 4H, cation 1/8-C<u>H</u> and cation DMAP *m*-C<u>H</u>), 6.59 (dd, $^3J_{HH}$ = 8.0 Hz, $^4J_{HH}$ = 3.2 Hz, 2H, cation DMAP *m*-C<u>H</u>), 3.14 (s, 6H, cation NMe), 3.07 (s, 6H, cation NMe). ^{19}F NMR (377 MHz, 298 K, d_6-DMSO): δ −134.1 (d, $^3J_{FF}$ = 26 Hz, 2F, cation *o*-C_6F_5), −134.6 to −134.8 (m, 6F, cation *o*-C_6F_5 and anion *o*-C_6F_5), −157.4 (t, $^3J_{FF}$ = 22 Hz, 1F, cation *p*-C_6F_5), −160.2 (t, $^3J_{FF}$ = 21 Hz, 2F, anion *p*-C_6F_5), −160.6 (t, $^3J_{FF}$ = 21 Hz, 1F, cation *p*-C_6F_5), −163.0 to −163.2 (m, 2F, cation *m*-C_6F_5), −164.8 to −165.0 (m, 4F, anion *m*-C_6F_5), −165.7 to −165.8 (m, 2F, cation *m*-C_6F_5). ^{11}B NMR (128 MHz, 298 K, d_6-DMSO): δ 10.3 (s, anion), 6.3 (br s, cation). ^{13}C{^{1}H} NMR (126 MHz, 298 K, d_6-DMSO), partial: δ 156.2 (s, DMAP *p*-<u>C</u>), 141.8 (br s, anion 9/10-<u>C</u>), 138.2 (s, cation DMAP *o*-<u>C</u>H), 136.4 (s, cation DMAP *o*-<u>C</u>H), 132.0 (s, cation O−C−<u>C</u>), 131.9 (s, cation O−C−C-<u>C</u>), 130.8 (s, cation 3/6-<u>C</u>H), 129.1 (s, cation 2/7-<u>C</u>H), 128.2 (s, cation 1/8-<u>C</u>H), 125.5 (br s, anion 2/7-<u>C</u>H), 124.5 (br s, anion O−C−C−<u>C</u>), 124.1 (s, cation 4/5-<u>C</u>H), 123.9 (br s, anion O−C−<u>C</u>), 123.0 (br s, anion 4/5-<u>C</u>H), 121.8 (br s, anion 3/6-<u>C</u>H), 119.7 (br s, anion 1/8-<u>C</u>H), 107.7 (s, cation DMAP *m*-<u>C</u>H), 107.2 (s, cation DMAP *m*-<u>C</u>H), 97.7 (cation O−<u>C</u>). N-Me ^{13}C resonances overlap with the residual solvent peak (see SI Figure 61). Elemental analysis calcd (%) for $C_{66}H_{36}B_2F_{20}N_4O_4$: C 58.69; H 2.69; N 4.15. Found: C58.17; H 2.71; N 3.99. $\lambda_{(abs)}$: 425 nm (CH_2Cl_2, $\varepsilon = 2.3 \times 10^4$ M^{-1} cm^{-1}), 473 nm (CH_2Cl_2, $\varepsilon = 9 \times 10^3$ M^{-1} cm^{-1}).

X-ray Data Collection, Reduction, Solution, and Refinement. A single crystal of **2** was coated in paratone-N oil and mounted. The data were collected using the SMART software package on a Siemens SMART System CCD diffractometer using a graphite monochromator with Mo Kα radiation (λ = 0.71073 Å). Data reduction was performed using the SAINT software package, and an absorption correction was applied using SADABS. The structures were solved by direct methods using XS and refined by full-matrix least-squares on F^2 using XL as implemented in the SHELXTL suite of programs. All non-hydrogen atoms were refined anisotropically. Carbon-bound hydrogen atoms were placed in calculated positions using an appropriate riding model and coupled isotropic temperature factors.

■ ASSOCIATED CONTENT

Supporting Information

The Supporting Information is available free of charge on the ACS Publications website at DOI: 10.1021/jacs.6b11190.

Experimental characterization data for the compounds (PDF)

Crystallographic data for compounds **5**, **6**, **7a**, **7b**, **8a**, **8b**, **9**, **10**, **11**, **13**, **14**, and **15** (ZIP)

■ AUTHOR INFORMATION

Corresponding Author

*dstephan@chem.utoronto.ca

ORCID

Douglas W. Stephan: 0000-0001-8140-8355

Author Contributions

The manuscript was written through contributions of all authors. All authors have given approval to the final version of the manuscript.

Notes

The authors declare no competing financial interest.

Full metrical parameters for the solid-state structures of compounds **5**, **6**, **7a**, **7b**, **8a**, **8b**, **9**, **10**, **11**, **13**, **14**, and **15** are available free of charge from the Cambridge Crystallographic Data Centre under reference CCDC 1511375−1511386, respectively.

■ ACKNOWLEDGMENTS

D.W.S. gratefully acknowledges the financial support of NSERC of Canada, the award of a Canada Research Chair. L.E.L. is grateful for the support of scholarships from NSERC and Digital Specialty Chemicals. The authors acknowledge the

DOI: 10.1021/jacs.6b11190
J. Am. Chem. Soc. 2017, 139, 426−435

Canadian Foundation for Innovation, project number 19119, and the Ontario Research Fund for funding of the Centre for Spectroscopic Investigation of Complex Organic Molecules and Polymers. Dr. Timothy Johnstone is gratefully acknowledged for X-ray crystallographic assistance and insightful discussions.

REFERENCES

(1) Gomberg, M. *J. Am. Chem. Soc.* **1900**, *22*, 757.
(2) *Stable Radicals: Fundamentals and Applied Aspects of Odd-Electron Compounds*; Hicks, R. G., Ed.; John Wiley & Sons Ltd: West Sussex, U.K., 2010.
(3) Odian, G. *Principles of Polymerization*; Wiley: Hoboken, NJ, 2004.
(4) Curran, D. P. *Synthesis* **1988**, *1988*, 417−419.
(5) Curran, D. P. *Synthesis* **1988**, *1988*, 489−513.
(6) Tang, X.; Wilson, S. R.; Solomon, K. R.; Shao, K.; Madronich, S. *Photochem. Photobiol. Sci.* **2011**, *10*, 280−291.
(7) Madronich, S.; Shao, M.; Wilson, S. R.; Solomon, K. R.; Longstreth, J. D.; Tang, X. Y. *Photochem. Photobiol. Sci.* **2015**, *14*, 149−169.
(8) Hayyan, M.; Hashim, M. A.; AlNashef, I. M. *Chem. Rev.* **2016**, *116*, 3029−3085.
(9) Power, P. P. *Chem. Rev.* **2003**, *103*, 789−809.
(10) Ji, L.; Griesbeck, S.; Marder, T. B. *Chem. Sci.* **2016**, DOI: 10.1039/C6SC04245G.
(11) Kaim, W.; Schulz, A. *Angew. Chem., Int. Ed. Engl.* **1984**, *23*, 615−616.
(12) Lichtblau, A.; Kaim, W.; Stahl, T.; Schulz, A. *J. Chem. Soc., Perkin Trans. 2* **1992**, *2*, 1497−1501.
(13) Schulz, A.; Kaim, W. *Chem. Ber.* **1989**, *122*, 1863−1868.
(14) Ji, L.; Edkins, R. M.; Lorbach, A.; Krummenacher, I.; Bruckner, C.; Eichhorn, A.; Braunschweig, H.; Engels, B.; Low, P. J.; Marder, T. B. *J. Am. Chem. Soc.* **2015**, *137*, 6750−6753.
(15) Elschenbroich, C.; Kühlkamp, P.; Behrendt, A.; Harms, K. *Chem. Ber.* **1996**, *129*, 859−869.
(16) Olmstead, M. M.; Power, P. P. *J. Am. Chem. Soc.* **1986**, *108*, 4235−4236.
(17) Kwaan, R. J.; Harlan, C. J.; Norton, J. R. *Organometallics* **2001**, *20*, 3818−3820.
(18) Berndt, A.; Klusik, H.; Schlüter, K. *J. Organomet. Chem.* **1981**, *222*, c25−c27.
(19) Emslie, D. J. H.; Piers, W. E.; Parvez, M. *Angew. Chem., Int. Ed.* **2003**, *42*, 1252−1255.
(20) Venkatasubbaiah, K.; Zakharov, L. N.; Kassel, W. S.; Rheingold, A. L.; Jäkle, F. *Angew. Chem., Int. Ed.* **2005**, *44*, 5428−5433.
(21) Chiu, C. W.; Gabbai, F. P. *Angew. Chem., Int. Ed.* **2007**, *46*, 1723−1725.
(22) Aramaki, Y.; Omiya, H.; Yamashita, M.; Nakabayashi, K.; Ohkoshi, S.; Nozaki, K. *J. Am. Chem. Soc.* **2012**, *134*, 19989−19992.
(23) Rosenthal, A. J.; Devillard, M.; Miqueu, K.; Bouhadir, G.; Bourissou, D. *Angew. Chem., Int. Ed.* **2015**, *54*, 9198−9202.
(24) Braunschweig, H.; Krummenacher, I.; Mailander, L.; Pentecost, L.; Vargas, A. *Chem. Commun.* **2016**, *52*, 7005−7008.
(25) Hoefelmeyer, J. D.; Gäbbai, F. P. *J. Am. Chem. Soc.* **2000**, *122*, 9054−9055.
(26) Scheschkewitz, D.; Amii, H.; Gornitzka, H.; Schoeller, W. W.; Bourissou, D.; Bertrand, G. *Science* **2002**, *295*, 1880−1881.
(27) Hubner, A.; Kaese, T.; Diefenbach, M.; Endeward, B.; Bolte, M.; Lerner, H. W.; Holthausen, M. C.; Wagner, M. *J. Am. Chem. Soc.* **2015**, *137*, 3705−3714.
(28) Bissinger, P.; Braunschweig, H.; Damme, A.; Kupfer, T.; Krummenacher, I.; Vargas, A. *Angew. Chem., Int. Ed.* **2014**, *53*, 5689−5693.
(29) Bissinger, P.; Braunschweig, H.; Damme, A.; Horl, C.; Krummenacher, I.; Kupfer, T. *Angew. Chem., Int. Ed.* **2015**, *54*, 359−362.
(30) Martin, C. D.; Soleilhavoup, M.; Bertrand, G. *Chem. Sci.* **2013**, *4*, 3020−3030.
(31) Kawamoto, T.; Geib, S. J.; Curran, D. P. *J. Am. Chem. Soc.* **2015**, *137*, 8617−8622.
(32) Ueng, S. H.; Solovyev, A.; Yuan, X.; Geib, S. J.; Fensterbank, L.; Lacôte, E.; Malacria, M.; Newcomb, M.; Walton, J. C.; Curran, D. P. *J. Am. Chem. Soc.* **2009**, *131*, 11256−11262.
(33) Walton, J. C.; Brahmi, M. M.; Monot, J.; Fensterbank, L.; Malacria, M.; Curran, D. P.; Lacôte, E. *J. Am. Chem. Soc.* **2011**, *133*, 10312−10321.
(34) Lavallo, V.; Canac, Y.; Prasang, C.; Donnadieu, B.; Bertrand, G. *Angew. Chem., Int. Ed.* **2005**, *44*, 5705−5709.
(35) Kinjo, R.; Donnadieu, B.; Celik, M. A.; Frenking, G.; Bertrand, G. *Science* **2011**, *333*, 610−613.
(36) Bertermann, R.; Braunschweig, H.; Dewhurst, R. D.; Horl, C.; Kramer, T.; Krummenacher, I. *Angew. Chem., Int. Ed.* **2014**, *53*, 5453−5457.
(37) Bissinger, P.; Braunschweig, H.; Damme, A.; Krummenacher, I.; Phukan, A. K.; Radacki, K.; Sugawara, S. *Angew. Chem., Int. Ed.* **2014**, *53*, 7360−7363.
(38) Ménard, G.; Hatnean, J. A.; Cowley, H. J.; Lough, A. J.; Rawson, J. M.; Stephan, D. W. *J. Am. Chem. Soc.* **2013**, *135*, 6446−6449.
(39) Cardenas, A.; Culotta, B.; Warren, T.; Grimme, S.; Stute, A.; Fröhlich, R.; Kehr, G.; Erker, G. *Angew. Chem., Int. Ed.* **2011**, *50*, 7567−7571.
(40) Liedtke, R.; Scheidt, F.; Ren, J.; Schirmer, B.; Cardenas, A. J. P.; Daniliuc, C. G.; Eckert, H.; Warren, T. H.; Grimme, S.; Kehr, G.; Erker, G. *J. Am. Chem. Soc.* **2014**, *136*, 9014−9027.
(41) Sajid, M.; Kehr, G.; Wiegand, T.; Eckert, H.; Schwickert, C.; Pottgen, R.; Cardenas, A. J. P.; Warren, T. H.; Fröhlich, R.; Daniliuc, C. G.; Erker, G. *J. Am. Chem. Soc.* **2013**, *135*, 8882−8895.
(42) Sajid, M.; Stute, A.; Cardenas, A. J. P.; Culotta, B. J.; Hepperle, J. A. M.; Warren, T. H.; Schirmer, B.; Grimme, S.; Studer, A.; Daniliuc, C. G.; Frohlich, R.; Petersen, J. L.; Kehr, G.; Erker, G. *J. Am. Chem. Soc.* **2012**, *134*, 10156−10168.
(43) Tao, X.; Kehr, G.; Wang, X.; Daniliuc, C. G.; Grimme, S.; Erker, G. *Chem.−Eur. J.* **2016**, *22*, 9504−9507.
(44) Turkyilmaz, F.; Kehr, G.; Li, J.; Daniliuc, C. G.; Tesch, M.; Studer, A.; Erker, G. *Angew. Chem., Int. Ed.* **2016**, *55*, 1470−1473.
(45) Longobardi, L. E.; Liu, L.; Grimme, S.; Stephan, D. W. *J. Am. Chem. Soc.* **2016**, *138*, 2500−2503.
(46) Holthausen, M. H.; Bayne, J. M.; Mallov, I.; Dobrovetsky, R.; Stephan, D. W. *J. Am. Chem. Soc.* **2015**, *137*, 7298−7301.
(47) Xu, B.-H.; Kehr, G.; Fröhlich, R.; Wibbeling, B.; Schirmer, B.; Grimme, S.; Erker, G. *Angew. Chem., Int. Ed.* **2011**, *50*, 7183−7186.
(48) Rahman, M. M.; Liu, H.-Y.; Eriks, K.; Prock, A.; Giering, W. P. *Organometallics* **1989**, *8*, 1−7.
(49) Green, S. P.; Jones, C.; Stasch, A. *Chem. Commun.* **2008**, 6285−6287.
(50) Sasaki, S.; Yoshifuji, M. *Curr. Org. Chem.* **2007**, *11*, 17−31.
(51) Grimme, S.; Brandenburg, J. G.; Bannwarth, C.; Hansen, A. *J. Chem. Phys.* **2015**, *143*, 054107.
(52) Furche, F.; Ahlrichs, R.; Hättig, C.; Klopper, W.; Sierka, M.; Weigend, F. *WIREs Comput. Mol. Sci.* **2014**, *4*, 91−100.

DOI: 10.1021/jacs.6b11190
J. Am. Chem. Soc. 2017, 139, 426−435